# A crustal profile across the Archaean Pilbara and northern Yilgarn cratons, northwest Australia

*B. J. Drummond*

**Two Archaean cratons are exposed in the Precambrian shield of Western Australia: the Pilbara in the north and the Yilgarn in the south. They are separated by the Capricorn Orogen. Seismic recordings of quarry blasts in the north of the West Australian shield indicate that the upper crustal rocks have seismic velocities of 6.0 km $s^{-1}$, and are probably of acid to intermediate chemical composition. They overlie a lower crust, presumed to be granulitic, which has a seismic velocity of 6.4 km $s^{-1}$ at 13 km depth in the north of the Pilbara Craton and 16 km in the north of the Yilgarn Craton. The northern Yilgarn has a third layer, with a seismic velocity of about 7.0 km $s^{-1}$, at the base of the crust. This may represent a higher grade (eclogite?) phase, or it may indicate injection of basic material into the base of the crust. The crust-mantle boundary at the base of the Pilbara Craton and Capricorn Orogen appears to be transitional—it shows velocity gradients rather than a first-order velocity discontinuity.**

**Within the Pilbara Craton, the crust is about 28 km thick in the north and 33 km in the south. South of the Pilbara Craton, the crust thickens under the Capricorn Orogenic Belt, and again under the northern Yilgarn Craton where it is 52 km thick. The form of the structures in the zone of thickening cannot be determined uniquely from the present data. Three models incorporating faults or monoclines and a wedge of 7.0 km $s^{-1}$ material at the base of the crust have been derived. The different crustal thicknesses of the cratons suggest that they formed separately and were then tilted towards the Orogenic Belt.**

## Introduction

The Precambrian shield is exposed over much of Western Australia. The shield region has both economic and scientific importance. In the north, twenty-five minerals have been reported in economic proportions (The Pilbara Study Group, 1974). The most abundant is iron ore, now mined and exported in considerable quantities. In addition, the geology and geochemistry of the Archaean areas of the shield are being extensively studied by the Geological Survey of Western Australia, CSIRO, BMR and various Australian universities.

BMR carried out a seismic refraction and gravity survey in the region in 1977 to investigate the structures of the crust and upper mantle in the region, and if possible, to shed light on the tectonic processes which influenced the formation of the early crust in the area.

Seven open-cut iron ore mines in the region regularly fire large quarrying blasts; these were used as energy sources for the seismic survey. One specially prepared blast was also used. Lines of portable seismographs were established along traverses which crossed most of the major geological provinces in the region. Gravity readings were made along many of the roads in the area.

This paper presents the results of the interpretation of the seismic data from one traverse. The gravity data, and the data from the other traverses are being processed and will be published elsewhere.

## Geology

The survey area (Fig. 1) may be divided geologically into two Archaean cratons—the Pilbara and Yilgarn Cratons—separated by the Hamersley, Bangemall and Nabberu Basins and the Gascoyne Province (Trendall, 1975a), which define the Proterozoic Capricorn Orogenic Belt (Gee, in press).

The Pilbara Block contains the oldest isotopically dated rocks in Australia (Pidgeon, 1978a). They are

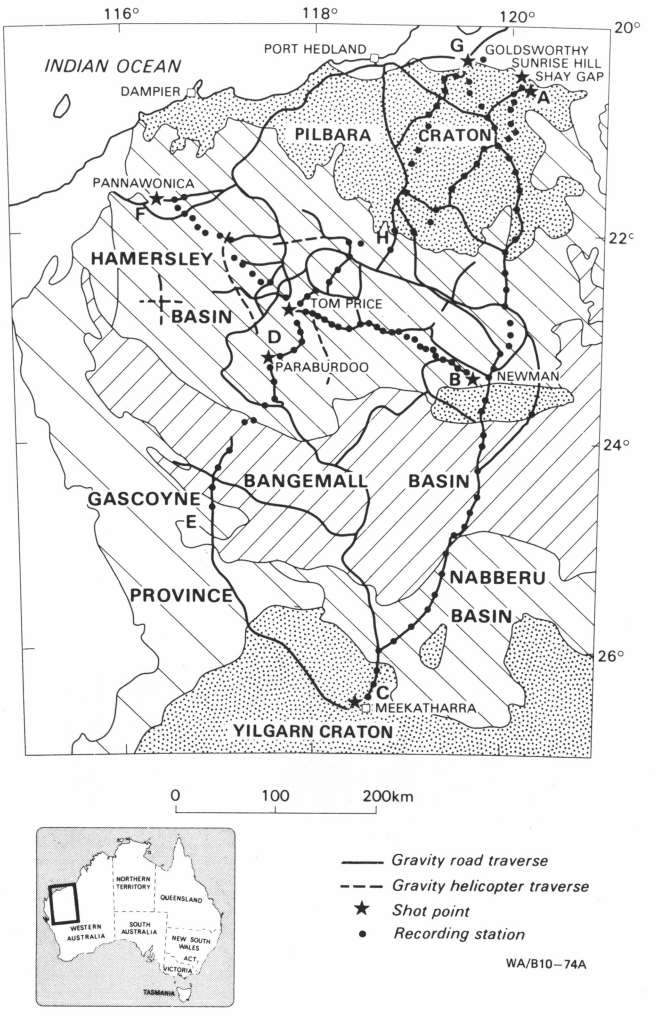


**Figure 1. Geology and survey design.**

volcanic and sedimentary rocks which are intruded by and overlap large granitoid batholiths (Blockley, 1975). The batholiths contain several phases of granites. The isotopic ages of the granites range from 2700 to 3400 m.y. (De Laeter & Blockley, 1972; De Laeter & others, 1975; Oversby, 1976; Pidgeon, 1978b; Hallberg & Glikson, in press).

Granites and greenstone successions also make up the stratigraphy of the Yilgarn Block; in the central and eastern, and northwestern parts of the block, the greenstone belts have distinct trends—NNW-SSE, and NNE-SSW, respectively (cf elsewhere in the Yilgarn, and the Pilbara). This is reflected in the regional gravity and magnetic patterns (BMR 1975a, 1975b). The southwest of the Yilgarn Block is a high-grade granulite terrain containing only remnants of the supracrustal succession. Isotopic ages of the granites in the Yilgarn Block range from 2500 to 2800 m.y. (Arriens, 1971; Oversby, 1975).

Overlapping the southern part of the Pilbara Block are early Proterozoic sediments and volcanics of the Hamersley Basin (Trendall, 1975b). The sediments and volcanics form three groups: the lowermost Fortescue Group, with volcanic rocks interspersed with sediments, the Hamersley Group, with large, basin-wide accumulations of banded iron formations, and the Wyloo Group which was restricted to a rapidly subsiding sub-basin in the south of the Hamersley Basin.

The sediments in the north of the Hamersley Basin dip southwards at a few degrees. South of the axis of the basin, the dips are to the north and become steeper until, near the southern boundary of the basin, the folding is intense and dips close to the vertical are common. In places, overturning to the north occurs. The Hamersley Basin sediments are variably metamorphosed. In the north, the metamorphism is prehnite-pumpellyite facies, increasing southwards to amphibolite facies in the Gascoyne Province (Horwitz & Smith, 1978).

On the southern side of the Capricorn Orogenic Belt, the sediments of the Nabberu Basin unconformably overlap the Yilgarn Craton (Hall & Goode, 1978). In the south of the basin, the sediments are predominantly sub-horizontal to gently dipping to the north. Farther north, the intensity of folding and the metamorphic grade increases. In the north and northwest of the basin, the folding is intense and the Archaean basement is increasingly included in the deformation (Hall & Goode, 1978). The metamorphic grade reaches granulite facies in the west.

In the west of the survey area, the Gascoyne Province (Daniels, 1975a) contains migmatised Archaean (?) rocks and remnants of the Wyloo and younger Bangemall Groups; the rocks are extensively faulted and folded, and metamorphic grade is variable.

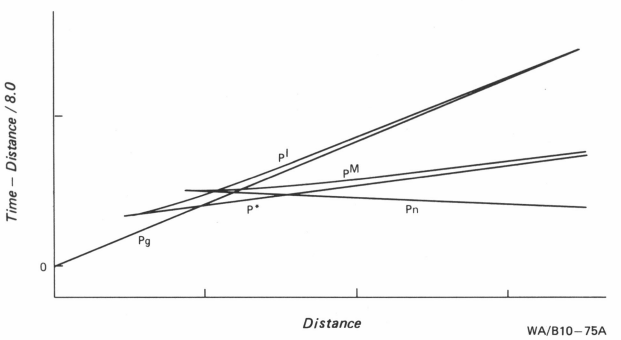


**Figure 2. Principal wave groups.**

The rocks of the Bangemall Basin (Daniels, 1975b) are mostly fine-grained sediments, but there are some conglomerates, breccias, tuffaceous sandstones and acid volcanics. They are the youngest Precambrian rocks in the area, unconformably overlying the rocks of the Hamersley and Nabberu Basins.

Since the deposition of the Bangemall Group, the area has been a positive landmass; it is mostly covered by Tertiary and Quaternary sand and soil.

## The crustal survey

The field work undertaken in 1977 will be described in detail by Drummond (in preparation) and only a summary is given here. The positions of the seismic stations are superimposed on the geological map (Fig. 1).

Only 15 recorders were used as mobile stations. Consequently, not all of the sites on any line could be occupied simultaneously. Equipment was moved along the lines after sufficient blasts had been recorded at each site; 137 seismic stations were occupied. One hundred and fifteen quarry blasts at seven iron ore mines within the region were used as seismic sources. A blast was specially prepared and fired in a disused mine shaft near Meekatharra.

Traverse ABC, interpreted in this paper, crossed the Pilbara Block, Hamersley, Bangemall and Nabberu Basins and the northern Yilgarn Block. Goldsworthy, Shay Gap and Sunrise Hill blasts were used as sources in the north, Newman blasts as sources in the centre. The Meekatharra blast was used to reverse the recordings of Newman blasts along line BC. Station spacing was generally about 20 km, but less near the blast sites.

## Seismic data processing

The recording stations used BMR-designed slow-speed seismic tape recorders. Two channels of vertical seismic data, at gain levels 24 db apart, as well as internal clock and radio-time signals, were recorded. The seismic traces for on-line shots along line ABC were digitised and record sections prepared for interpretation. Representative data from line ABC are presented in Figure 3.

Differing nomenclature is used in the literature to describe the wave groups commonly observed in crustal seismic investigations. The nomenclature used here is modified from that of Giese (1976). Figure 2 is a diagrammatic time-distance graph showing the principal wave groups observed in the Pilbara region.

Pg waves are refracted through the crystalline basement. In the Pilbara region, they generally occur as first arrivals to about 130 km, and have phase velocities of about 6 km $s^{-1}$. P* waves are refracted through the lower crust. Giese (1976) does not differentiate this phase from the Pg wave group. They are seldom observed as first arrivals, and have velocities of around 6.4 km $s^{-1}$. $P^I$ waves are supercritical (wide-angle) reflections from the lower crustal layer. Pn waves penetrate the uppermost part of the mantle. They occur as first arrivals beyond about 130 km and have velocities generally greater than 8 km $s^{-1}$. $P^M$ waves are supercritical reflections from the Moho.

Shots with clearly recorded codas were used to build composite record sections shown for lines ABC and GBC in Figure 3. Amplitudes were not normalised for shot weights, recorder gains or distance. The traces have been filtered digitally in the bandpass 0.5 to

| *Source and direction* | | *Phase* | *Velocity km s⁻¹* | *(Std error)* | *Intercept s* | *(Std error)* | *RMS residual s* | *No. of points* |
|---|---|---|---|---|---|---|---|---|
| Goldsworthy | South | Pg | 6.01 | (0.02) | 0.03 | (0.05) | 0.11 | 26 |
| Goldsworthy | South | Pn[1] | 8.20 | (0.05) | 5.92 | (0.17) | 0.16 | 17 |
| Goldsworthy | South | Pn[2] | 8.52 | (0.04) | 7.40 | (0.23) | 0.11 | 11 |
| Sunrise Hill | South | Pg | 6.01 | (0.02) | 0.18 | (0.04) | 0.10 | 23 |
| Shay Gap | South | Pg | 6.05 | (0.02) | 0.19 | (0.04) | 0.11 | 27 |
| Shay Gap | South | Pn | 8.18 | (0.11) | 5.68 | (0.40) | 0.18 | 6 |
| Newman | North | Pg | 5.86 | (0.04) | —0.13 | (0.09) | 0.20 | 20 |
| Newman | North | Pn | 8.49 | (0.05) | 6.99 | (0.17) | 0.18 | 18 |
| Newman | South | Pg | 6.08 | (0.04) | 0.04 | (0.10) | 0.23 | 20 |
| Newman | South | Pn[3] | 8.46 | (0.07) | 7.73 | (0.19) | 0.08 | 7 |
| Newman | South | Pn[4] | 7.25 | (0.05) | 2.75 | (0.31) | 0.10 | 9 |
| Meekatharra | North | Pg | 6.12 | (0.02) | 0.17 | (0.06) | 0.10 | 11 |
| Meekatharra | North | Pn | 8.68 | (0.11) | 10.60 | (0.58) | 0.31 | 6 |
| Meekatharra | South | Pn | 8.08 | (0.03) | 6.37 | (0.22) | 0.11 | 7 |

**Table 1. Velocities and intercepts along line ABC, from linear regression analyses.**

1. Data north of Newman; 2. Data south of Newman; 3. Data between 175 and 255 km; 4. Data beyond 255 km.

8.0 Hz. The arrival times of the principal wave groups were determined from analog chart records. The travel times were then calculated and the apparent phase velocities and intercepts determined by least squares linear regression analysis.

A summary of the results from the regression analysis appears in Table 1. The analysis was applied mainly to first-arrival data, although some second and subsequent arrivals were included when their onsets could be defined. Consequently, only Pg and Pn phases were considered. The velocities and intercepts of the P* phase were scaled directly from the record sections.

## Interpretation methods

For interpretation, line ABC was split into segments AB and BC. Most interpretative methods, e.g. the Reciprocal Method (Hawkins, 1961), the Time-Term Method (Scheidegger & Willmore, 1957) and the method described by Ewing & others (1938), Dooley (1952), and Mota (1954), require reversed travel-time data. The data along line ABC are not usually reversed. Along the segment AB, Pg occurs as first arrivals to about 130 km, and Pn as first arrivals beyond 130 km. Because the segment is about 330 km long, Pg arrivals are reversed only for the sections of the line where they occur as second or subsequent arrivals whose onset times are poorly defined. The Pn phase from either end of the traverse bottoms in different parts of the upper mantle and is therefore not truly reversed. The P* phase has poor timing because it is never a first arrival.

The Reciprocal and Time-Term methods, which are based on the discrete travel-times from the shots to the stations, are therefore inappropriate to interpret the data along line AB, and also along segment BC, where similar considerations apply. However, the third method mentioned above is based on the apparent velocities and intercept times of the seismic energy in both directions along the lines. If it is assumed that similar phases at either end of each segment of the line are reciprocal pairs, and the refractors are continuous between the shots, this method can be used to derive plane-layered models, which provide the basis for further modelling.

The depths, dips and velocities of the refractors under the shot points were calculated. The Pn data for segment BC could not be assumed to be reversed, and other assumptions, discussed later, were made. The models derived from the inversion of the seismic data were then modelled using ray-tracing techniques and the models adjusted to fit the record sections in Figure 3. Several models are shown in Figure 4. Their upper crustal features along segments AB and BC, and their lower crustal features along segment AB are similar; their crust/mantle boundary features along segment BC are different. The travel time curves derived from the models are superimposed on the record sections in Figure 3.

## Seismic interpretation

The record sections (Fig. 3) present some of the data recorded along line ABC; in most cases high-gain recordings are shown. Second and subsequent arrivals are sometimes seen more clearly on the low-gain traces or on recordings of other shots. The following descriptions of the record sections therefore refer to the entire data set, and not just the records shown in Figure 3. The record sections are reduced travel-time plots. The factor (Distance/8.0) has been subtracted from the time axis for each trace. In the following discussion, reduced travel-times are quoted.

### *Line AB (and GB)—Goldsworthy to Newman*

Figure 3a shows recordings of Goldsworthy blasts southwards along line GBC. Recordings beyond 500 km were poor and are not shown. Pg phases occur as first arrivals to about 130 km, and can be traced farther as second and subsequent arrivals. They have an apparent phase velocity of 6.01 km $s^{-1}$, and an almost zero intercept time (Table 1). Because velocities of about 6 km $s^{-1}$ are representative of crystalline basement, the near zero intercept indicates that the basement is very close to the surface. The $P^*/P^I$ cusp is best observed on a low-gain trace at about 90 km. The cusp may occur closer to the blast, but the over-modulation on closer recordings obscures the true nature of the traces. A velocity of 6.4 km $s^{-1}$ and an intercept of 1.0 s were assigned to the P* phase. Large amplitude phases in the 6 to 8 s range between 120 and 200 km are interpreted as $P^M$ arrivals. The $P^M$/Pn cusp occurs in over-moduled coda at about 80 km and 6s. Pn is observed as first arrivals beyond 140 km. The Pn phase between Goldsworthy and Newman has a velocity of 8.20 km $s^{-1}$ and an intercept of 5.92 s. South of Newman, the Pn velocity increases slightly (Table 1), although the point at which this occurs is difficult to define.

Record sections of Shay Gap and Sunrise Hill blasts southwards along line AB show similar travel-time features (Fig. 3b), but because these blasts are smaller than at Goldsworthy the amplitudes of the traces are smaller. Although this obscures some of the more

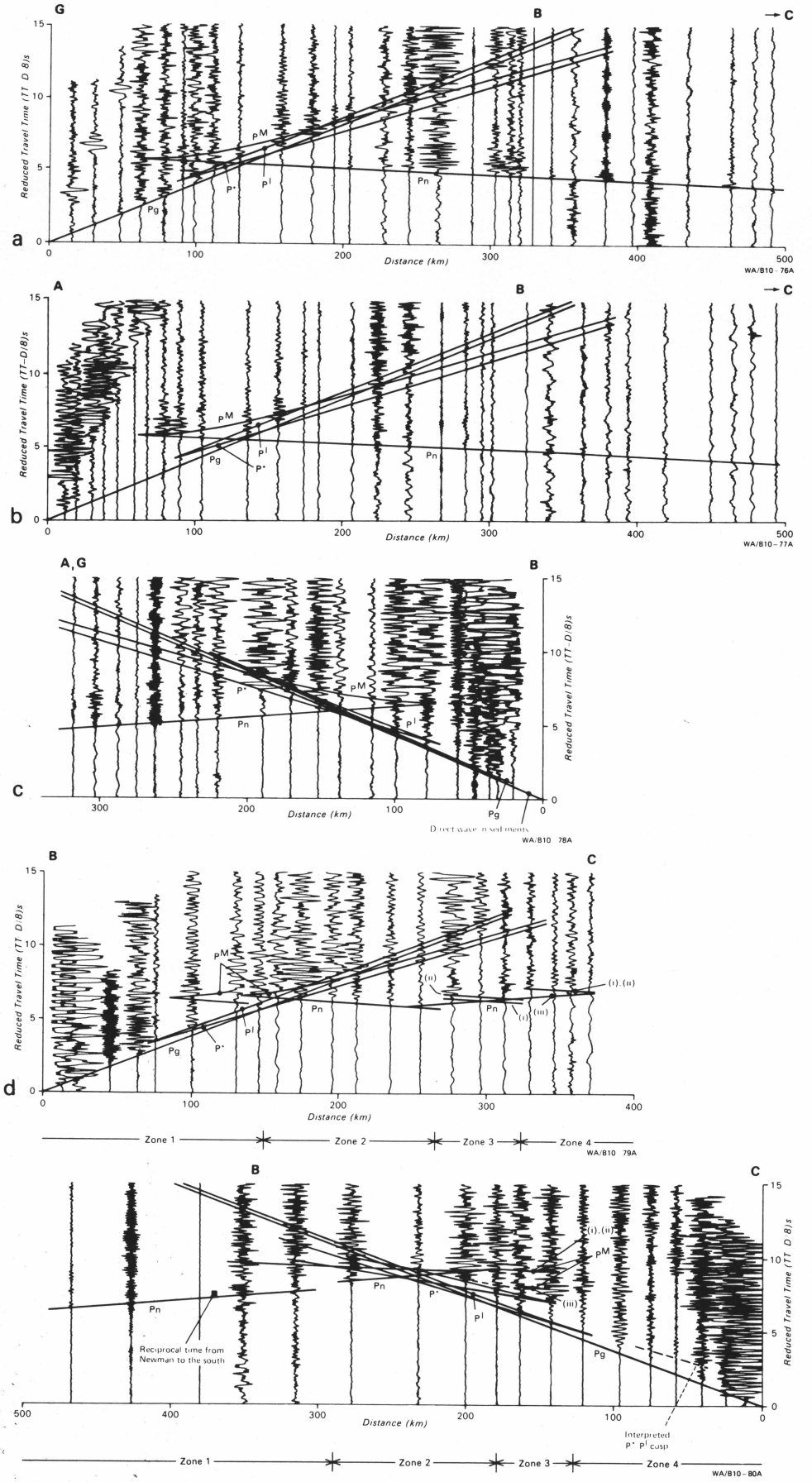


**Figure 3. Records sections along line ABC. The travel time curves superimposed on the record sections in 3a, 3b, and 3c were calculated for the model in Figure 4a. In 3d and 3e, the travel time curves numbered i, ii and iii are for the models in Figures 4a, 4b and 4c respectively.**

emergent arrivals, it allows better definition of the $P^M$ wavegroup and the $P^M$/Pn cusp. The velocities and intercepts are similar to those from the Goldsworthy data (Table 1).

Newman blasts recorded northwards along line AB are shown in Figure 3c. They had large areal extents, with blasting on benches several kilometres apart making up one shot, and very long burning times, with delays sometimes totalling over a second. The Newman shots therefore often produced very emergent arrivals.

The Pg phase velocity, as measured from first arrivals, is 5.86 km $s^{-1}$. This is lower than that derived from Goldsworthy, Shay Gap and Sunrise Hill blasts, and also from south of Newman and north of Meekatharra. It could be caused by either the emergent arrivals, whose onsets were picked later than they in fact occur, or the sediments of the Hamersley Basin, which crop out in the region; the sediments are often iron-rich, metamorphosed, and have compressional wave velocities in hand specimens approaching those of the crystalline basement (Drummond, in preparation). The Pg phase has a slightly negative intercept time (Table 1), indicating a decrease in apparent velocity and therefore density away from the shots. This is consistent with increasing thicknesses of sedimentary rocks to the north of Newman.

The P* phase appears to be present, but its velocity and intercept were difficult to determine because of the unclear nature of the onsets. An apparent phase velocity of 6.4 km $s^{-1}$ and intercept of 1 s were adopted, although the velocity could be as high as 6.45 km $s^{-1}$ and the intercept as large as 1.65 s. The upper surface of the lower crustal layer was therefore interpreted as horizontal, although its depth could increase southwards from Goldsworthy to Newman by as much as 5 km.

The Pn phase northwards from Newman is quite clear, and has a phase velocity of 8.49 km $s^{-1}$ and intercept time of 6.99 s. The Pn arrivals from Newman northwards seem to have two phases, separated by 0.6 s. To demonstrate this, traces from two shots have been plotted in Figure 3c, one between 160 and 250 km and the other beyond 250 km. The arrivals out to 250 km have a low-frequency phase followed by one of higher frequency. Beyond 250 km both phases have high frequencies, although the second phase is only clear on the trace at 300 km. The duality of the arrivals may be caused by source effects, because traces from different shots have different waveforms. Alternatively, because it may also be interpreted on some traces of Goldsworthy blasts in Figure 3a (see for example the traces at 230, 240, and 340 km), it may be caused by a complex velocity-depth function at the crust/mantle boundary; this interpretation is supported by large amplitude arrivals in the 6 to 8s range between 80 and 200 km, which do not readily fit the $P^M$ wave group as modelled. The large amplitude phases are not present in the Goldsworthy data.

The simplest interpretation of the data from segment AB is that the crust is two-layered; the upper layer has a seismic P-wave velocity of 6.0 km $s^{-1}$, and the lower layer a velocity of 6.4 km $s^{-1}$. The lower layer has a horizontal interface at 13 km depth, but it may dip from about 9 km under Goldsworthy to 14 km under Newman. The crust/mantle boundary dips from 28 km in the north to about 33 km in the south. The upper mantle velocity is 8.34 km $s^{-1}$ (Fig. 4). A layer of sediments north of Newman may be incorporated into the

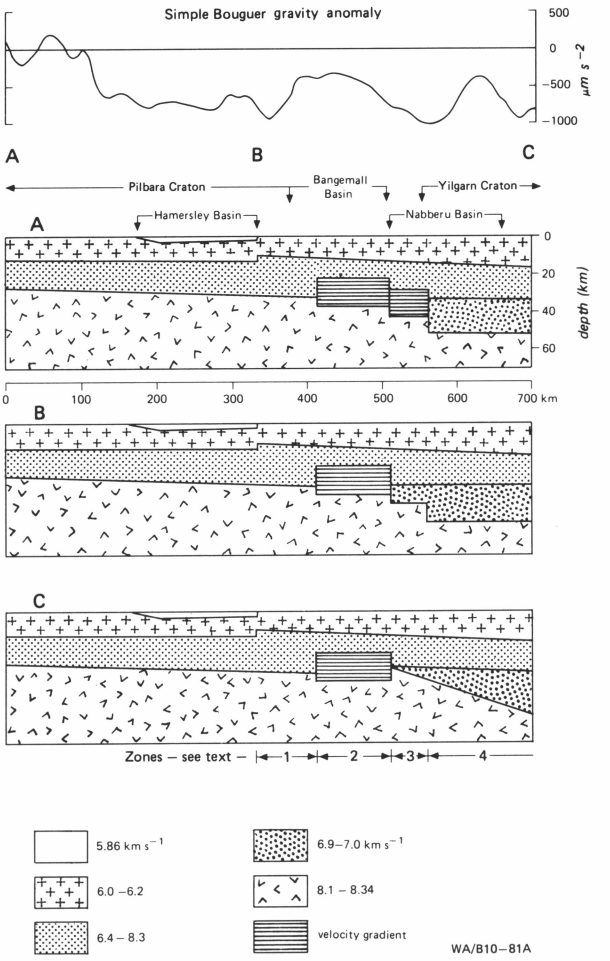


**Figure 4. Gravity profile and seismic crustal models along line ABC.**

model to explain the low upper crustal velocity from the Newman data. Trendall (1975b) shows diagrammatically that a maximum thickness of 2 to 3 km of Hamersley Basin sediments is likely to the north of Newman. Incorporation of the sediments into the model does not significantly perturb the theoretical travel-times.

The travel-time curves superimposed on the record sections (Fig. 3a, 3b, and 3c) were calculated using ray-tracing techniques on section AB of the model in Figure 4a. The model is satisfactory for first-arrival data, and for the Pg phase. However, the fit of the model travel-times to the reflected phases, and particularly the $P^M$ phase, is not satisfactory. The $P^M$ phase is about 1 s earlier than the time-distance curve for the model. This indicates that velocity gradients, in which the velocity increases with depth, may be present at the base of the crust. A gradient at the base of the crust will draw the $P^M$ phase closer to the Pn phase. This is demonstrated in Figure 5 by modelling the Goldsworthy, Sunrise Hill, and Shay Gap with a plane, horizontal layered model with the velocity/depth function shown in Figure 5a. The function has a linear increase in velocity from 6.4 km $s^{-1}$ to 8.20 km $s^{-1}$ over a depth range of 15 km at the base of the crust. The $P^M$ phase now fits the observed curve more closely than in Figures 3a and 3b, but the $P^M$/Pn cusp is not so well modelled.

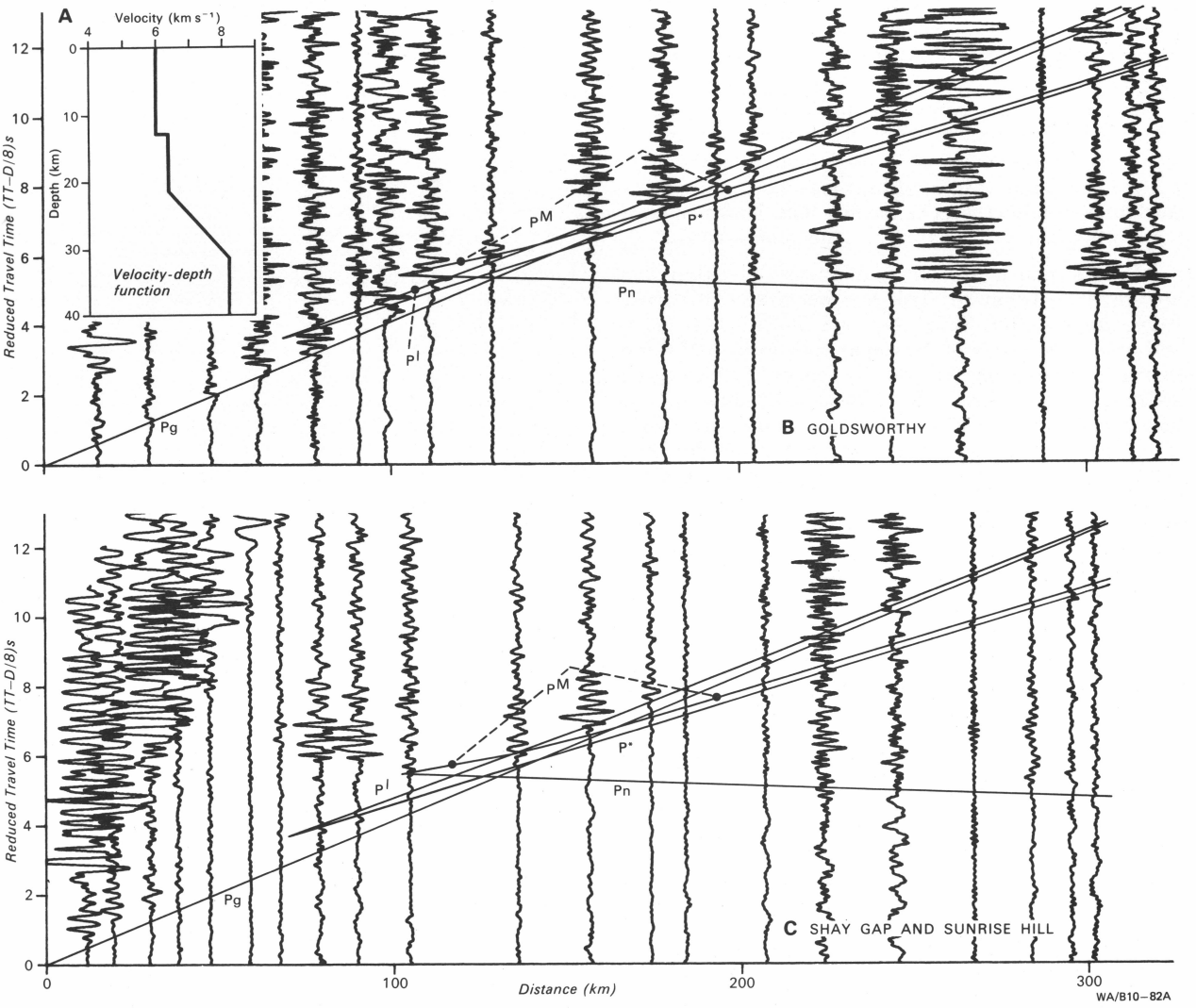


**Figure 5. Effects of a velocity gradient at the crust/mantle boundary along line AB.**

*Line BC—Newman to Meekatharra*

South of Newman, the Pg velocity is 6.08 km $s^{-1}$ (Fig. 3d, Table 1) and the intercept is close to zero. At about 70 km, the Pg phase seems to disappear, to be replaced about 0.5 s later by another set of arrivals with a phase velocity of 6.4 km $s^{-1}$ and an intercept of 1 s. The disappearance of the Pg phase may be owing to spreading of the wavefronts. However, it may also have several other causes, for example the crystalline basement may be downfaulted south of Newman. This does not seem unreasonable in view of other anomalies in the record section to be discussed later. A step of 0.5 s represents a throw on the fault of over 8 km. The step in the travel times may also be caused by a low velocity zone in the upper crust. Both of these causes, however, require low density material in the upper crust in the region of a high gravity anomaly (Fig. 4). Consequently, because of the similarity of its velocity and intercept time to those for the P* group north of Newman, the wave group beyond 75 km has been interpreted as the P* phase.

Beyond 170 km, the first arrivals are the Pn wave group, which has a phase velocity of 8.46 km out to 250 km, beyond which it abruptly decreases to 7.25 km $s^{-1}$ and the Pn arrivals are increasingly delayed. Several interpretations are possible. The Moho may have a change in dip. For a two-layered crust, with seismic velocities similar to those along segment AB, overlying a mantle with a seismic velocity of 8.3 km $s^{-1}$, a change in dip of 6 degrees is sufficient to account for the abrupt change in the apparent velocity of the Pn phase. Alternatively, two steps in the travel-time curve, of the type expected from fault-like structures, may be interpreted at 260 and 320 km, implying three regions at the crust/mantle boundary separated by fault-like structures.

Large-amplitude arrivals in the 7 to 9 s range between 100 and 280 km are interpreted as the $P^M$ wave group. Difficulties in fitting the interpreted $P^M$/Pn cusp to the apparent Pn curve between 170 and 240 km, and fitting the curve $P^M$ reflections to all of the observed arrivals have required the interpretation of a third step in the Pn travel-time curve at 130 km, implying a fourth region in the crust/mantle boundary defined by a fault-like structure. This is supported by the record section from Meekatharra.

To describe the features observed in the Meekatharra blast data (Fig. 3e) in terms of the features on the Newman record section (Fig. 3d), four zones have been defined (Fig. 3d and 3e). They do not correspond to the same regions on the surface in the two record sections because the crust is thicker in the south of segment BC.

Zone 1 extends about 80 km south of Newman. Zones 2 and 3 are about 100 and 50 km long respectively, and Zone 4 extends about 140 km north from Meekatharra. When the appropriate offsets are applied to the groups of reflection phases on the two record sections, they are shown to bottom in the same zones.

In Figure 3e (the Meekatharra blast data), the Pg phase is emergent and has a velocity of 6.12 km $s^{-1}$. A slightly higher value of 6.18 km $s^{-1}$ was eventually adopted for modelling purposes because it provided a better fit to some later arrivals. The P* phase has a velocity of 6.4 km $s^{-1}$ and an intercept of 1.65 s. A lower crustal reflected phase, defined by a suite of large amplitude arrivals at about 7 to 8 s between 140 and 200 km, was also interpreted. No refracted phase could be uniquely defined for this group, but a velocity of 7.0 km $s^{-1}$ and an intercept of about 5 s were derived by drawing a tangent to the reflected phase at the interpreted cusp. The $P^M$/Pn cusp occurs at about 10 s and 140 km; it is more obvious on the low-gain traces than the high-gain traces plotted. At about 200 km, the interpreted Pn phase velocity increases slightly, and at about 300 km a step, corresponding to the zone 1/zone 2 boundary inferred in the Newman data (Fig. 3d), occurs in the travel-time data. The Pn velocity of 8.68 km $s^{-1}$ corresponding to the zone 1 section of the Moho is greater than that observed from Newman blasts recorded northwards (8.49 km/s).

If the features in the record sections along segment BC were caused by the effects of vertical velocity structure, the record sections from Newman southwards and Meekatharra northwards would be similar. However, because of the obvious differences, the features cannot be explained in terms of vertical velocity structure; they must be caused by lateral structures within the crust and upper mantle. The following procedure was therefore followed to interpret and model the segment BC. The Pg and P* phases recorded south from Newman and north from Meekatharra have similar velocities, so the upper and lower crustal layers with velocities of 6.1 and 6.4 km $s^{-1}$ respectively were assumed to be continuous between the two blasting centres. This assumption is necessary, because no information is available about the upper crust in the centre of the profile. The lower crustal layer, responsible for the P* refractions of 6.4 km $s^{-1}$ velocity, was modelled as being 10 km deep under Newman and 16 km deep under Meekatharra (Fig. 4a and c).

The model immediately to the north of Newman, without the sedimentary basin, was extended southwards for 80 km. This corresponds to the point at which the Pg phase dies out (Fig. 3d); the model also satisfies the Pn data from the Meekatharra blast. 80 km south of Newman, a delay of 0.4 s observed in the Pn data was interpreted as indicating a deepening of the Moho by 4 km to about 37 km (Fig. 4a, b and c). No information about the true velocities is available; therefore, the lower crustal layers south of this point were assumed to be horizontal, and the estimates of the apparent velocity were used as the true velocities. To fit the reflections more closely, a gradient was necessary at the base of the crust in zone 2. That adopted was a linear increase in velocity from 6.4 km $s^{-1}$ to 8.3 km $s^{-1}$ over a 15 km depth range. In zones 3 and 4, several models fit the data. The Moho may have fault or monocline-type structures, with a thickening of the crust by about 6 km at the zone 2/zone 3 boundary, and a further thickening at the zone 3/zone 4 boundary of 9 km to 52 km under Meekatharra (Fig. 4a and b). The nature of the material at the base of the crust in zone 3 cannot be defined from the data available. The model in Figure 4a has a velocity gradient, and the model in Figure 4b has 7.0 km $s^{-1}$ material. Alternatively, the crust/mantle boundary may have a change of dip, with a wedge of 7.0 km $s^{-1}$ material at the base of the crust (Fig. 4c). The theoretical travel times for the right-hand sides (segment BC) of the models in Figure 4 have been superimposed on the record sections in Figures 3d and 3e; the fit is generally good. However, the $P^M$ times for one model (Fig. 4c) are about 1 s earlier than recorded in Figure 3e. The times south from Newman for this model are also slightly early. The model could be made to fit the data by simply thickening the southern end of the lower crustal wedge of 7.0 km $s^{-1}$ material. However, making the crust too thick might be difficult to explain geologically, isostatically, and tectonically because of the crustal thicknesses to the north under the Pilbara Craton and under the southern Yilgarn Craton (Mathur, 1974; Mathur & others 1977).

Another feature of the travel-time data not well modelled is the interpreted $P^*/P^I$ cusp north from Meekatharra (Fig. 3c). The cusp derived from the model does not extend far enough back towards the origin.

*Composite model along profile ABC*

When the models for segments AB and BC were adjusted to give a close fit of the theoretical times to the data from each segment (within 0.2 s for first arrival data), they were joined and further tested by modelling the travel times for Goldsworthy blasts south of Newman. The curvature in the observed travel times beyond Newman was also present in the modelled times, although to a lesser extent, with deviations of the modelled times from the measured times of up to 0.3 a. Unfortunately, the arrivals beyond 500 km were generally poor and the models could not be tested more exhaustively.

The models in Figure 4 may be summarised as follows. An upper crustal layer of 6.0 km $s^{-1}$ is present at the surface along the profile, except to the north of Newman where the Hamersley Basin sediments crop out, and perhaps 80 km to the south of Newman, where a thick pile of low-velocity rocks may occur. A lower crustal phase, with a velocity of 6.4 km $s^{-1}$, is observed at all shot points, and is refracted from a crustal layer 9 to 13 km deep under Goldsworthy, Shay Gap, and Sunrise Hill, and 16 km deep under Meekatharra. The step in the refractor under Newman in the models results from the process in which segments AB and BC were interpreted independently. It is probably not real, and the refractor is probably continuous between Goldsworthy and Meekatharra. This would make the calculated travel times from the full model fit the Goldsworthy arrivals beyond Newman more closely. The crust is 28 km thick near the northern mines, and thickens to 33 km about 80 km to the south of Newman, where it abruptly thickens to 37 km, and a velocity gradient is probably present at the base of the crust. One hundred kilometres farther south, the crust again thickens. The lower crust may be a wedge of 7.0 km $s^{-1}$ material or the crust/mantle boundary may have several faults or monoclines.

The upper mantle velocity along segment AB is 8.34 km $s^{-1}$. Along segment BC, 8.3 km $s^{-1}$ was adopted in zones 2, 3 and 4 in the models in Figures 4a and 4b; 8.34 km $s^{-1}$ was used in zone 1. Gregson (1978)

reported the arrival times of the Meekatharra blast energy at the seismological observatories up to 700 km to the south on the Yilgarn Craton. Using a revised origin time slightly different to the preliminary one Gregson used, an apparent velocity of 8.08 km $s^{-1}$ and an intercept time of 6.37 s were calculated for the Pn phase across the Yilgarn Craton. The intercept time is considerably less than that for Meekatharra blast data to the north, implying that this is an up-dip velocity, so that the true velocity is probably lower. The effect of earth curvature would also increase the apparent velocity when measured over such large distances, so that the true velocity is probably somewhat less than 8.08 km $s^{-1}$. The apparent velocity (8.08 km $s^{-1}$) was used as the velocity in the upper mantle in zones 3 and 4 in the model in Figure 4c.

## Discussion

The boundaries between the zones in the models in Figure 4 have so far been referred to as "fault-like structures". No information is available about the true nature of these structures; only their sense is apparent; in all cases the deeper side of the crust/mantle boundary is to the south. Their width must be less than the station spacing, which is about 20 km along line BC. The geological map of Australia (BMR, 1976) shows that the line crossed two major faults, one of which corresponds to the zone 2/zone 3 boundary. The zone 1/zone 2 boundary corresponds to a fault zone reported by Brakel & Muhling (1976). R. E. Smith (CSIRO, personal communication, 1979) calls it the Mount Vernon-Brumby Creek Fault, and reports that it continues for 200 km. The zone 1/zone 2 and zone 2/zone 3 boundaries therefore correspond to the known surface expressions of major faults. The zone 3/zone 4 boundary does not.

The Proterozoic sedimentary basins were not convincingly observed in the seismic data. A sedimentary basin 2 to 3 km thick was included in the model north of Newman without having to adjust the depths of the other refractors in the model by more than a kilometre. Perturbations that could be related to Bangemall Basin sediments may be interpreted in the Pg data south of Newman.

The southern limit of the Bangemall Basin outcrop area corresponds to the zone 2/zone 3 boundary, but the northern edge of the basin outcrop area is offset about 40 km to the north of the zone 1/zone 2 boundary. The basin has a broad 600 um $s^{-2}$ gravity high centred over it (Fig. 4). Because the seismic velocities imply uniform densities in the upper crust, the transition zone at the base of the crust must represent denser crustal material than on either side of the zone. This interpretation is supported by Wellman (1978), who predicted on gravity evidence that the Capricorn Orogenic Belt between the Archaean cratons had a thicker, more dense crust than the cratons. Because the only lateral density differences in the seismic models occur at the base of the crust, it can also be inferred that the velocity gradient proposed at the crust-mantle boundary under the Pilbara Block is not as broad as the one at the base of zone 2.

The Nabberu Basin is interpreted from the geology as overlapping the northern edge of the Yilgarn Block, and its northern limits seem to correspond fairly well with the zone 2/zone 3 boundary. It may be that the tectonism which folded the sediments and the Archaean basement of the Nabberu Basin (Hall & Goode, 1978) also left its imprint on the lower crust in the form of seismically anomalous material at the base of the crust in zone 3.

The Pilbara Block is interpreted as extending 80 km south of Newman. This is about 30 km farther south than implied by the outcrop of Archaean granite inliers in the Hamersley Basin. The Yilgarn Block is interpreted from the geology as extending northwards under the Nabberu Basin to include granite inliers of supposed Archaean age. This is in fairly close agreement with the zone 3/zone 4 seismic boundary.

### *Crustal composition*

Hickman & Lipple (1975) presented diagrammatic cross-sections of the crust in the northeastern part of the Pilbara Block. Presumably based on the structure of the greenstone belts and on the foliation patterns in the granites, the sections show the granites and the synclinal keels of the greenstone belts extending to 30 km depth. Their models imply that the crust is likely to have an average acid to intermediate composition. Ringwood (1975) predicted that a purely basaltic lower crust was unlikely because, in a region of low heat flow, a dry mafic lower crust in thermodynamic equilibrium would exist as eclogite and have seismic P-wave velocities of about 8.4 km $s^{-1}$. Ringwood's favoured model for the lower crust in old, stable regions is one of acid to intermediate chemical composition, composed principally of granulites and eclogites with seismic P velocities in the range 6.5 to 7.2 km $s^{-1}$.

The interpretation of lower crustal material as granulites is supported by Tarney & Windley (1977), and Dawnson (1977), although they favour some basification of the lower crust in continental areas. The velocity of 6.4 km $s^{-1}$ in the lower crustal layer in the Pilbara and Yilgarn Blocks is slightly less than that expected for Ringwood's model; a velocity gradient at the base of the crust would bring the models closer to agreement.

Glikson & Lambert (1976) proposed, in agreement with the model of Hickman and Lipple (1975), that the granite to greenstone ratio increases with depth in the Pilbara and Yilgarn Cratons. They also predicted an increase in the metamorphic grade to amphibolite, and even granulite facies, with depth. The lower crust may therefore be more acidic than Ringwood (1975), Tarney & Windley (1977), and Dawson (1977) predicted; this would account for the lower observed velocities.

The seismic data in th e Pilbara Block are therefore consistent with a crust of average acid to intermediate chemical composition, with a transition, probably from amphibolite to granulite, at about 13 km.

The transition to granulite is also present in the northern Yilgarn Block, although it is slightly deeper. It is underlain at about 30 km by a third crustal layer with a velocity of about 7.0 km $s^{-1}$. Mathur (1974) interpreted the crustal structure along several seismic and gravity profiles in the southern Yilgarn Block. He also derived a three-layer crustal model, although his lower crustal velocities of 7.3 to 7.5 km $s^{-1}$ were higher than in the models in Figure 4. Glikson & Lambert (1976) found Mathur's lower most crustal layer anomalously dense, and suggested that it might result from the accumulation of basic magmas at the crust-mantle boundary during the break up of Gondwanaland. Tarney & Windley (1977) favour a mechanism whereby the crust becomes chemically stratified during its creation. The mafic material. being dense, is restricted to the lower crust. The velocities in the north

of the Yilgarn Block are lower than the southern values, and are consistent with Ringwood's (1975) model. The simpler explanation of the lowermost crustal layer being caused by further phase changes, perhaps to eclogite grade, of a thick, somewhat chemically stratified crust with the increased pressure and temperature likely at the base of a thick crust, is attractive. It eliminates the need to invoke a tectonic mechanism for injecting basic material into the base of the entire Yilgarn Block, but not the Pilbara Block.

*Structural development*

Palaeomagnetic data (McElhinny & McWilliams, 1977; Embleton, 1978) imply that the Pilbara and Yilgarn Blocks are unlikely to have formed at widely separated locations and subsequently been brought closer together by plate-tectonic movements.

However, they do not rule out the possibility that the blocks may have formed as one craton which was later rifted, as proposed by Horwitz & Smith (1978). The present data cannot define the nature of the crust in the Capricorn Orogenic Belt with sufficient clarity to determine whether it represents an ancient rift system. However, the different thicknesses of the cratons and the divergent isotopic ages for the rocks within the cratons tend to imply separate development of the cratons in their approximate relative positions.

Glikson & Lambert (1976) suggested that the arcuate style of the greenstone belts and the generally greater isotopic ages of the granites of the Pilbara Block indicated that the rocks formed at a deeper level of the crust than the rocks to the south in the Yilgarn Block. They were subsequently uplifted and exposed by erosion. This has now been discounted by Hallberg & Glikson (in press), but requires further investigation in the light of different crustal thicknesses in the Pilbara and northern Yilgarn Cratons.

The seismic model indicates that the base of the Pilbara Block has a dip to the south. A. Y. Glikson (BMR, personal communication, 1979) suggested that the increasing granite-greenstone ratio northwards across the Pilbara Craton, as evidenced by the largely granite terrains in the north of the survey area, is further evidence of southerly dip. The dip from the seismic modelling is about the same as the dip observed in the Hamersley Basin sediments over the craton, implying that the entire craton was tilted to the south following the deposition of the sediments.

The base of the Yilgarn Craton has been shown (Fig. 4) as either horizontal (Fig 4a and b) or dipping steeply to the south (Fig. 4c). The survey data do not allow a unique interpretation of the dip and these dips were assumed in the interpretation. They are presented here as possible models for the northern part of the Yilgarn Craton. The intercept times of the Meekatharra blast data to the north and south, and the presence of a higher grade lower crustal granulite terrain in the southwest of the Yilgarn Craton (Glikson & Lambert, 1976) suggest that the dips in Figure 4 are local features and that, overall, the Yilgarn Craton as a structural unit has been tilted to the northeast. The tilting occurred after the deposition of the Nabberu Basin sediments, which dip northwards on the Yilgarn Craton.

The Pilbara and Yilgarn Cratons therefore seem to have developed separately in their approximate relative positions, and were tilted towards their common mobile belt, the Capricorn Orogenic Belt, after the deposition of the lower and middle Proterozoic sediments in the mobile belt.

## Acknowledgements

The BMR is indebted to the iron-mining companies of the Pilbara without whose support the seismic survey would not have been possible. The staff of Goldsworthy Mining Limited, Cliffs Robe River Associates, Hamersley Iron Pty Ltd, and Mount Newman Mining Company Pty Ltd gave of their own time on several occasions to make the survey a success.

I acknowledge the efforts of my colleagues at the BMR who undertook the field work during 1977, and their support and comments during the interpretation of the data. The interpretation was undertaken while I was a full-time research scholar at the Australian National University (ANU) in receipt of an Australian Public Service Board Postgraduate Scholarship. I thank the staff and students of the ANU, and particularly K. J. Muirhead and J. Cleary, whose guidance and comments were most useful. A. Y. Glikson critically read the manuscript and made many useful comments and suggestions. The figures were drawn by M. Moffat.

## References

ARRIENS, P. A., 1971—The Archaean geochronology of Australia. *Geological Society of Australia, Special Publications,* **3**, 11-23.

BLOCKLEY, J. G., 1975—Pilbara Block. *In* Geology of Western Australia. *Western Australia Geological Survey, Memoir* **2**, 81-93.

BMR, 1975a—Gravity map of Australia, 1:5 000 000. *Bureau of Mineral Resources, Geology & Geophysics, Canberra, Australia.*

BMR, 1975b—Magnetic map of Australia, 1:2 500 000 (4 sheets). *Bureau of Mineral Resources, Geology & Geophysics, Canberra, Australia.*

BMR, 1976—Geology of Australia, 1:2 500 000 (4 sheets). *Bureau of Mineral Resources, Australia, Canberra.*

DANIELS, J. L., 1975a—Gascoyne Province. *In* Geology of Western Australia. *Western Australia Geological Survey, Memoir* **2**, 107-14.

DANIELS, J. L., 1975b—Bangemall Basin. *In* Geology of Western Australia. *Western Australia Geological Survey, Memoir* **2**, 147-59.

DAWSON, J. B., 1977—Sub-cratonic crust and upper mantle models based on xenolith suites in kimberlite and nephelinitic diatremes. *Journal of the Geological Society of London,* **134**, 173-84.

DE LAETER, J. R., & BLOCKLEY, J. G., 1972—Granite ages within the Archaean Pilbara Block, Western Australia. *Journal of the Geological Society of Australia,* **19**, 363-70.

DE LAETER, J. R., LEWIS, J. D. & BLOCKLEY, J. G., 1975—Granite ages within the Shaw Batholith of the Pilbara Block. *Geological Survey of Western Australia, Annual Report,* 1974, 73-9.

DOOLEY, J. C., 1952—Calculation of depth and dip of several layers by refraction seismic method. *In* THYER, R. F., & VALE, K. R., 1952—Geophysical Surveys, Oakland-Coorabin coalfield, New South Wales. *Bureau of Mineral Resources, Australia, Bulletin,* **19**.

BRAKEL, A. T. & MUHLING, P. C., 1976—Stratigraphy, sedimentation, and structure in the western and central part of the Bangemall Basin, Western Australia. *Geological Survey of Western Australia Annual Report,* 1975, 70-79.

DRUMMOND, B. J., 1979—Structural relations between the Archaean Pilbara and Yilgarn Blocks, Western Australia, from deep seismic sounding. *Australian National University, MSc. Thesis* (unpublished).

DRUMMOND, B. J., in preparation—Pilbara Crustal Survey, 1977—Operational Report. *Bureau of Mineral Resources, Australia, Record.*

EMBLETON, B. J. J., 1978—The palaeomagnetism of 2400 m.y. old rocks from the Australian craton and its relation to Archaean-Proterozoic tectonics. *Precambrian Research*, **6**, 275-91.

EWING, M., WOOLLARD, G. P., & VINE, A. C., 1938—Geophysical investigations in the emerged and submerged Atlantic coastal plain. *Bulletin of the Geological Society of America*, **50**, 257-95.

GEE, R. D., in press—Tectonics of the Western Australian Shield.

GIESE, P., 1976—Models of crustal structure and main wave groups. *In* GIESE, P., PRODEHL, C., & STEIN, A. (Editors) —Explosion seismology in Central Europe. Data and results. Crustal and upper mantle structure in Europe. *European Seismological Commission, Monograph*, **1**, *Springer-Verlag, Berlin*, 196-200.

GLIKSON, A. Y., & LAMBERT, I. B., 1976—Vertical zonation and petrogenesis of the early Precambrian crust in Western Australia. *Tectonophysics*, **30**, 55-89.

GREGSON, P. J., 1978—Mundaring Geophysical Observatory, Annual Report 1977. *Bureau of Mineral Resources, Australia, Record*, **1978/73**.

HALL, W. D. M., & GOODE, A. D. T., 1978—The early Proterozoic Nabberu Basin and associated iron formations of Western Australia. *Precambrian Research*, **7**, 129-84.

HALLBERG, J. A., & GLIKSON, A. Y., in press—Archaean granite-greenstone terrains of Western Australia. *In* HUNTER, D. R. (Editor)—Precambrian of the southern hemisphere. *Elsevier, Amsterdam.*

HAWKINS, L. V., 1961—The reciprocal method of routine shallow seismic refraction investigations. *Geophysics*, **26**, 806-19.

HICKMAN, A. H., & LIPPLE, S. L., 1975—Explanatory notes on the Marble Bar 1:250 000 geological sheet, Western Australia. *Geological Survey of Western Australia. Record*, **1974/20** (unpublished).

HORWITZ, R. C., & SMITH, R. E., 1978—Bridging the Yilgarn and Pilbara Blocks, Western Australia. *Precambrian Research*, **6**, 293-322.

MATHUR, S. P., 1974—Crustal structure in southwestern Australia from seismic and gravity data. *Tectonophysics*, **24**, 151-82.

MATHUR, S. P., MOSS, F. J., & BRANSON, J. C,. 1977—Seismic and gravity investigations along the Geotraverse, Western Australia, 1969. *Bureau of Mineral Resources, Australia, Bulletin* **191**.

MCELHINNY, M. W., & MCWILLIAMS, M. O., 1977—Precambrian geodynamics—a palaeomagnetic view. *Tectonophysics*, **40**, 137-59.

MOTA, L., 1954—Determination of dips and depths of geological layers by the seismic refraction method. *Geophysics*, **19**, 242-54.

OVERSBY, V. M., 1975—Lead isotope systematics and ages of Archaean acid intrusives in the Kalgoorlie-Norseman area, Western Australia. *Geochimica et Cosmochimica Acta*, **39**, 1107-25.

OVERSBY, V. M., 1976—Isotope ages and geochemistry of Archaean acid igneous rocks from the Pilbara, Western Australia. *Geochimica et Cosmochimica Acta*, **40**, 817-29.

PIDGEON, R. T., 1978a—3450 m.y. old volcanics in the Archaean layered greenstone succession of the Pilbara Block, Western Australia. *Earth and Planetary Science Letters*, **37**, 421-8.

PIDGEON, R. T., 1978b—Geochronological investigations of granite batholiths of the Archaean granite-greenstone terrain of the Pilbara Block, Western Australia. *In* SMITH, I. E. M., & WILLIAMS, J. G. (Editors)—Proceedings of the 1978 Archaean Geochemistry Conference. *University of Toronto*, 360-2.

RINGWOOD, A. E., 1975—COMPOSITION AND PETROLOGY OF THE EARTH'S MANTLE. *McGraw-Hill, New York.*

SCHEIDEGGER, A. E., & WILLMORE, P. L., 1957—The use of a least squares method for the interpretation of data from seismic surveys *Geophysics*, **22**, 9-22.

TARNEY, J., & WINDLEY, B. F., 1977—Chemistry, thermal gradients and evolution of the lower continental crust. *Journal of the Geological Society of London*, **134**, 153-72.

THE PILBARA STUDY GROUP, 1974—The Pilbara Study: Report on the industrial development of the Pilbara (to the Governments of Australia and Western Australia). *Australian Government Publishing Service, Canberra.*

TRENDALL, A. F., 1975a—Precambrian: Introduction. *In* Geology of Western Australia. *Western Australia Geological Survey, Memoir* **2**, 25-32.

TRENDALL, A. F., 1975b—Hamersley Basin. *In* Geology of Western Australia. *Western Australia Geological Survey, Memoir* **2**, 119-43.

WELLMAN, P., 1976—Regional variation of gravity, and isostatic equilibrium of the Australian crust. *BMR Journal of Australian Geology and Geophysics*, **1**, 297-302.

WELLMAN, P., 1978—Gravity evidence for abrupt changes in mean crustal density at the junction of Australian crustal blocks. *BMR Journal of Australian Geology and Geophysics*, **3**, 153-62.